Springer

Journal of Mechanical Science and Technology 23 (2009) 1620~1627

Journal of
Mechanical
Science and
Technology

www.springerlink.com/content/1738-494x
DOI 10.1007/s12206-008-1106-1

# Predicting performance of radial flow type impeller of centrifugal pump using CFD †

Suthep Kaewnai, Manuspong Chamaoot and Somchai Wongwises*

*Fluid Mechanics, Thermal Engineering and Multiphase Flow Research Lab. (FUTURE), Department of Mechanical Engineering, King Mongkut's University of Technology Thonburi, Bangmod, Bangkok 10140, Thailand*

(Manuscript Received August 31, 2006; Revised April 20, 2008; Accepted November 17, 2008)

**Abstract**

The main objective of this work is to use the computational fluid dynamics (CFD) technique in analyzing and predicting the performance of a radial flow-type impeller of centrifugal pump. The impeller analyzed is at the following design condition: flow rate of 528 $m^3$/hr; speed of 1450 rpm; and head of 20 m or specific speed ($N_s$) of 3033 1/min in US-Units. The first stage involves the mesh generation and refinement on domain of the designed impeller. The second stage deals with the identification of initial and boundary conditions of the mesh-equipped module. In the final stage, various results are calculated and analyzed for factors affecting impeller performance. The results indicate that the total head rise of the impeller at the design point is approximately 19.8 m. The loss coefficient of the impeller is 0.015 when $0.6 < Q/Q_{design} < 1.2$. Maximum hydraulic efficiency of impeller is 0.98 at $Q/Q_{design} = 0.7$. Based on the comparison of the theoretical head coefficient and static pressure rise coefficient between simulation results and experimental data, from previous work reported in the literature [Guelich, Kreiselpumpen, Springer, Berlin, 2004], it is possible to use this method to simulate the performance of a radial-flow type impeller of a centrifugal pump.

*Keywords*: Centrifugal pump; CFD; Impeller; Radial flow

## 1. Introduction

The use of CFD plays an important role in fluid mechanics. Due to the progress of numerical methods and computer capability, the impeller design for centrifugal pumps nowadays has been analyzed by using 3D-Navier stokes program or CFD software to predict impeller performance in advance. However, both the prediction and design cannot be done easily without sufficient information and experience. If the result from the CFD is much different from the designed value, the impeller could be redesigned before being put into real production.

Over the years, the application of CFD in fluid mechanics and turbomachinery has been studied by a number of researchers [1-8]. However there are few studies applying the CFD for predictions involving a radial flow type impeller. To the best of our knowledge to date, there have been only two works carried out by [9] and [10], in dealing with this issue.

[9] analyzed about 30 pump impellers having specific speeds between 12 to 160 (metric units) using a commercial 3D-Navier Stokes program for a standard k-ε turbulence model. The head and efficiency obtained from the software were compared to those obtained from the measurement. A set of rather stringent rules for the CFD calculations was developed in order to reduce the effect of grid and calculation parameters on the results.

[10] performed a 3D-CFD simulation of the impeller and volute of a centrifugal pump having a specific speed of 32 (metric units) and an outside impeller radius of 204.2 mm, by using CFX codes. A 3D flow simulation for the impeller with a structured grid was

† This paper was recommended for publication in revised form by Associate Editor Seungbae Lee
*Corresponding author. Tel.: +662 470 9115, Fax.: +662 470 9111
E-mail address: somchai.won@kmutt.ac.th

presented. A sensitivity analysis was done based on grid quality and various turbulence model. The final suitable impeller model was used for a 3D quasi-unsteady flow simulation of the impeller-volute stage. The flow simulation was performed for several impeller blades and volute tongue relative positions.

Although some information is currently available on applying the CFD for predicting of radial flow type impeller, there still remains room for further research. In the present study, the main concern is to

- predict theoretical head or theoretical head coefficient at any volumetric flow rate
- predict total head rise or total head coefficient of impeller at any volumetric flow rate
- predict impeller loss or impeller loss coefficient at any volumetric flow rate
- determine effect of turbulence model on total head rise of impeller
- examine uniformity of $C_{m2}$ distribution which affects the mixing losses (Q-H curve instability)
- elucidate the method to validate the CFD results

## 2. Impeller design process

Usually, there are two methods to design the impeller: direct method and inverse method. In the present study, the direct method is used. Fig. 1 shows the impeller design process which starts with specifications of the impeller by identifying flow rate, Q head, H and speed, n.

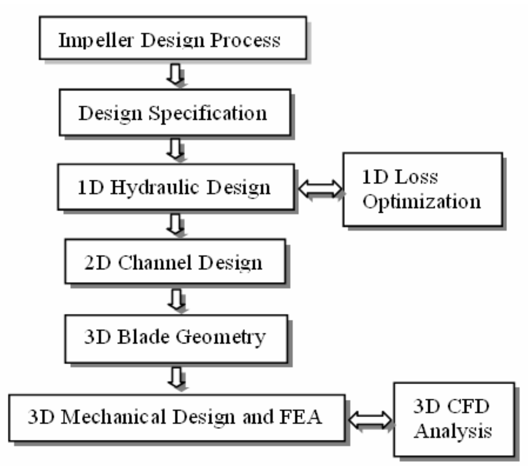


Fig. 1. Design process of impeller.

## 3. Mathematical model basic equation

In the present study the commercial CFD software CFX 5.5 was used. For three-dimensional incompressible and unsteady flow, the continuity equation and momentum equation in the rotating coordinate system are as follows:

Continuity equation

$$\frac{\partial \rho}{\partial t} + \vec{\nabla}.\rho \vec{V} = 0 \tag{1}$$

Momentum equation

$$\rho \frac{d\vec{V}}{dt} + \vec{\nabla} P = \rho \vec{g} + \mu\left(\nabla^2 . \vec{V}\right) - 2\rho \vec{\Omega} \times \vec{V} - \rho \vec{\Omega} \times \left(\vec{\Omega} \times \vec{r}\right) \tag{2}$$

## 4. Parameters in calculation of performance

In analyzing the impeller with CFD code, velocity and pressure at the control surface on the upstream and downstream side of the impeller can be integrated as follows:

- Static pressure rise coefficient of the impeller

$$\psi_P = \frac{2}{\rho U_2^2}\left(\overline{P_{2static}} - \overline{P_{1static}}\right) \tag{3}$$

- Total head rise coefficient

$$\psi_{LA} = \frac{2}{\rho U_2^2}\left(\overline{P_{2total}} - \overline{P_{1total}}\right) \tag{4}$$

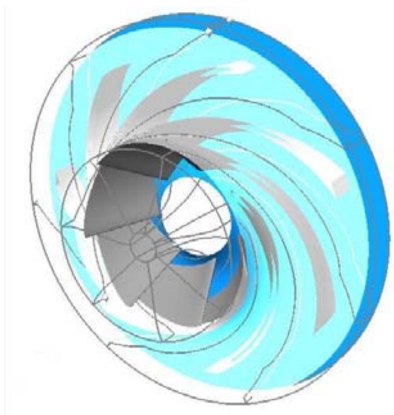

Fig. 2. 3D visualization of impeller.

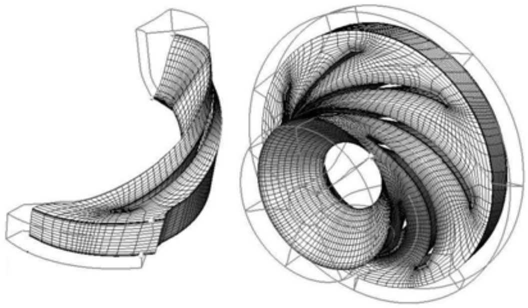

Fig. 3. Mesh on simulation domain.

• Theoretical head coefficient

$$\psi_{th} = 2\left(\frac{\overline{UC_{u2}}}{U_2^2} - \frac{\overline{UC_{u1}}}{U_2^2}\right) = \frac{2gH_{th}}{U_2^2} \quad (5)$$

• Hydraulic loss or loss coefficient of the impeller

$$\zeta_{LA} = \psi_{th} - \psi_{LA} = \frac{2gZ_{La}}{U_2^2} \quad (6)$$

• Hydraulic efficiency of the impeller

$$\eta_{h,impeller} = \frac{\psi_{LA}}{\psi_{th}} \quad (7)$$

or $$\eta_{h,impeller} = \frac{Total\ head\ rise}{Theoretical\ head}$$

## 5. Analysis of flow in the impeller

The impeller analysis for the radial flow centrifugal pump was based on these design details: speed of 1450 rpm; flow rate of 528 $m^3$/hr; head of 20 m or specific speed of 3033 1/min in US units. The dimension of the impeller is obtained as follows: impeller diameter, 300 mm; exit width, 42 mm; total number of blade impellers, 7; and angle at the exit, 24.5°. The impeller is as shown in Fig. 2. The analysis starts with the mesh generation and refinement on the domain. This mesh has a hexahedral shape as shown in Fig. 3. The analyzed parameters are shown in Table 1.

Table 1. Simulation.

| PARAMETERS | CFX 5.5 |
|---|---|
| Flow simulation domain | Single impeller flow channel |
| Mesh | Structured |
| Fluid | Water at 25 °C |
| Inlet | Total pressure = 101325 Pa |
| Outlet | Mass flow rate = variable (kg/s) |
| Wall | No slip |
| Turbulence model | k - ε , k - ω, RNG k - ε |
| Turbulence intensity | 1% , 5% , 10% |
| Maximum residual convergence | $10^{-4}$ (RMS) |

Table 2. Mesh details.

| Mesh | Number of node | Number of element | Minimum face angle | Maximum edge length ratio |
|---|---|---|---|---|
| A | 17340 | 14720 | 18.2653 | 68.7239 |
| B | 25080 | 21300 | 18.0644 | 71.7829 |
| C | 34200 | 29820 | 18.0644 | 51.6179 |
| D | 43320 | 38340 | 18.0644 | 58.7055 |
| E | 50440 | 44160 | 17.5859 | 88.2421 |
| F | 58200 | 51520 | 17.5859 | 71.8257 |
| G | 65960 | 58880 | 17.5859 | 64.5811 |
| H | 81480 | 73600 | 17.5859 | 50.8711 |
| I | 91500 | 81900 | 17.4755 | 90.5938 |

## 6. Results and discussion

### 6.1 Effect of number of mesh

Since the number of mesh nodes or openings affects the analysis, a suitable mesh number should be determined. Generally, a value of about 45,000 – 75,000 nodes is used in impeller analysis. In this work, nine models of mesh were constructed on domain to determine the effect from the mesh number, as shown in Table 2.

The analysis of flow in the impeller indicates that a mesh number in the range of 45,000 – 75,000 nodes yields similar results. However, to facilitate further study, the E model mesh was selected for the next analysis.

### 6.2 Effect of the change of the turbulence model

In CFD analysis, turbulence model should be selected. In this work, turbulence models (k - ε , k - ω ,

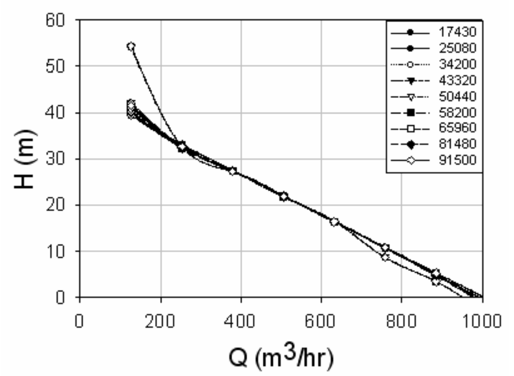


Fig. 4. Performance of impeller obtained from nine models of mesh.

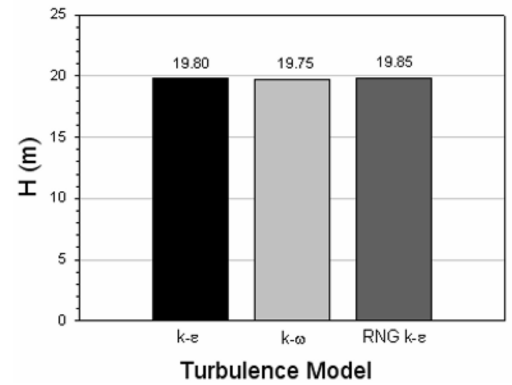


Fig. 5. Total head rise of impeller obtained from various turbulence models.

RNG k - ε) are selected to compare the use of various turbulence models on impeller performance. The analysis reveals that the head values gained from all three turbulence models are similar, with only 0.3% difference. However, the turbulence model k - ε is selected for further analysis.

### *6.3 Effect from the change of the turbulence intensity*

The change in turbulence intensity affects the impeller performance. In this work, three levels of turbulence intensity are used: 1%, 5%, and 10%. The analysis reveals that the head values gained from all three turbulence intensity levels are similar; however, 5 % was selected for further analysis.

### *6.4 Impeller performance*

From this study, the performance of a impeller could be determined as shown in Figs. 7-10. The head

Table 3. Performance parameters obtained from CFX 5.5.

| Parameter | | $\psi_p$ | $\psi_{th}$ | $\psi_{LA}$ | $\zeta_{LA}$ |
|---|---|---|---|---|---|
| Turbulence intensity | 1% | 0.1811 | 0.2107 | 0.1980 | 0.0127 |
| | 5% | 0.1810 | 0.2107 | 0.1979 | 0.0128 |
| | 10% | 0.1805 | 0.2106 | 0.1974 | 0.0132 |
| Surface roughness (mm) | 0 | 0.1809 | 0.2107 | 0.1979 | 0.0128 |
| | 1E-4 | 0.1810 | 0.2108 | 0.1980 | 0.0128 |
| | 1E-3 | 0.1812 | 0.2115 | 0.1984 | 0.0131 |
| | 0.01 | 0.1824 | 0.2163 | 0.2013 | 0.0150 |
| | 0.1 | 0.1834 | 0.2284 | 0.2068 | 0.0215 |

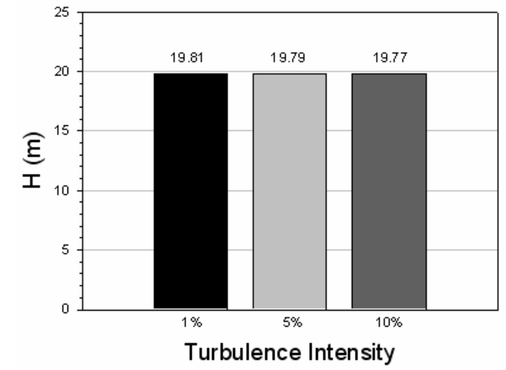


Fig. 6. Total head rise of impeller obtained from various turbulence intensity.

value determined at the design point is 20 m. Hence, it could be seen from Fig. 7 that the total head rise value of 19.8 m is nearly to the designed head. Fig. 8 shows the static pressure rise coefficient and theoretical head coefficient at different volumetric flow rates of the impeller. In real practice, it is quite difficult to measure the static pressure rise in experiments. From Fig. 9, it can be seen that a small amount of loss occurred in the impeller at the $Q/Q_{design}$ value within the range of 0.6-1.2. The loss coefficient at this range is around 0.015. This shows the high impeller efficiency and no recirculation. The performance of impeller decreases outside this range. At low volumetric flow rate, there is recirculation of water at the impeller inlet, starting at the $Q/Q_{design}$ value below 0.6. The hydraulic efficiency of the impeller is the ratio of total head coefficient and theoretical head coefficient, $\eta_h = \dfrac{\psi_{LA}}{\psi_{th}}$. From Fig. 10, the best hydraulic efficiency value is at $Q/Q_{design}$ = 0.7. The use of CFD software makes the hydraulic efficiency of the impeller prediction easier. Figs. 11-12 show meridian velocity at the impeller exit from hub to shroud. The

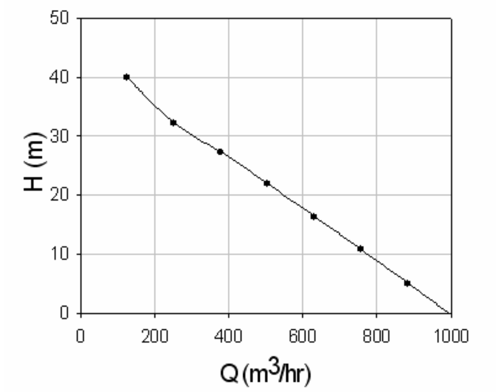


Fig. 7. Plot of total head rise against volumetric flow rate.

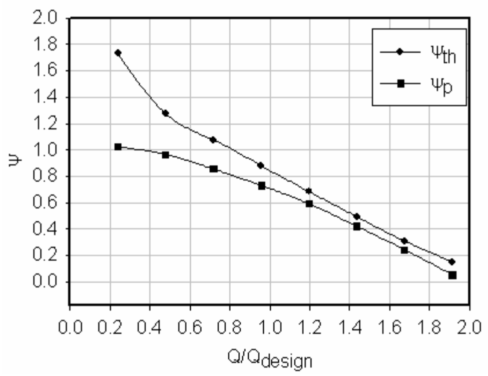


Fig. 8. Plot of static pressure coefficient and theoretical head coefficient against ratio of volumetric flow rate.

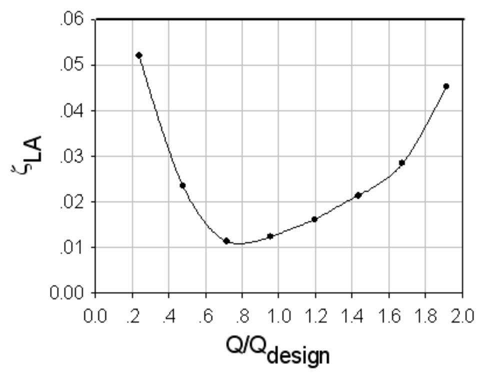


Fig. 9. Plot of loss coefficient against ratio of volumetric flow rate.

non-uniformity of the meridian velocity distribution affects the mixing losses and Q-H curve instability at low volumetric flow rate. This is unavoidable since the impeller revolved and produced friction at its surface. It can be seen from Table 3 that losses in the impeller increase with increasing surface roughness.

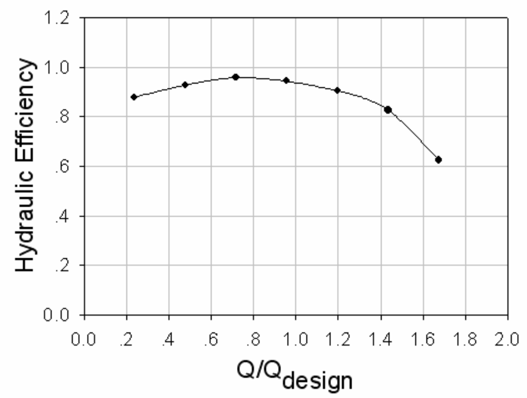


Fig. 10. Plot of hydraulic efficiency of the impeller against ratio of volumetric flow rate.

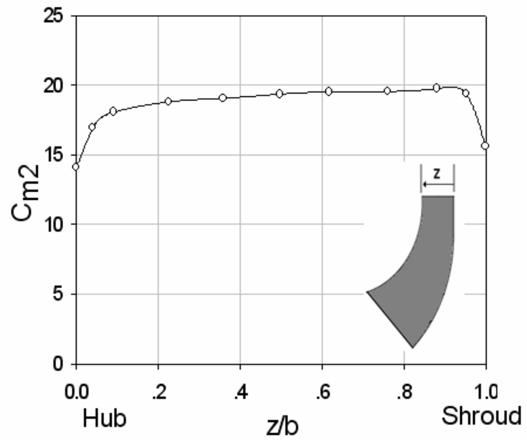


Fig. 11. Plot of meridian velocity at impeller exit.

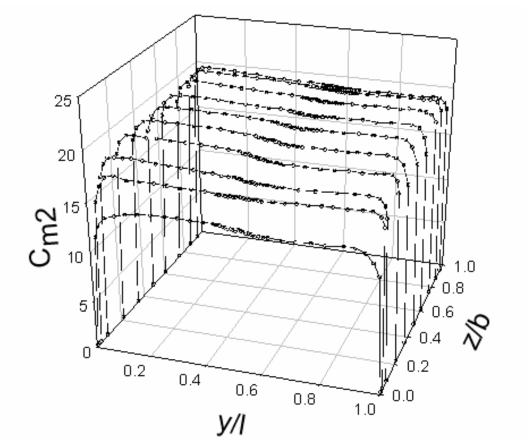


Fig. 12. Plot of meridian velocity at impeller exit in 3D.

## 7. Validation of CFD results

Simulation results can be validated by comparison with the experimental data. In this work, static pressure rise coefficient and theoretical head coefficient are the parameters that can be used for verification.

The static pressure rise can be obtained from the static pressure data taken from the pressure transducer installed on the surface of impeller at the inlet and outlet of pump. Then, the static pressure rise coefficient $\psi_{p,exp}$ calculated from $\psi_{p,exp} = \frac{2gH_p}{U_2^2}$ is compared with that obtained from Eq. (3).

The other parameter used to verify the simulation results is the theoretical head coefficient. The first step to derive this parameter starts from the hydraulic efficiency of pump, $\eta_{h,pump}$, obtained from

$$\eta_{h,pump} = \frac{1 + \frac{Q_{sp}}{Q} + \frac{Q_E}{Q} + \frac{Q_h}{Q}}{\frac{1}{\eta} + \frac{\sum P_{RR} + \sum P_{s3} + P_m + P_{er}}{P_w}} \tag{8}$$

where the water horse power, $P_w$ is calculated from

$$P_w = \rho g Q H_{tot} \tag{9}$$

where $\eta$, $H_{tot}$ and $Q$ are obtained from the performance curve of the pump.

Then, the theoretical head, $H_{tot}$, can be determined from $\eta_{h,pump} = \frac{H_{tot}}{H_{th}}$ and the theoretical head coefficient from $\psi_{th,exp} = \frac{2gH_{tot}}{\eta_{h,pump} U_2^2}$

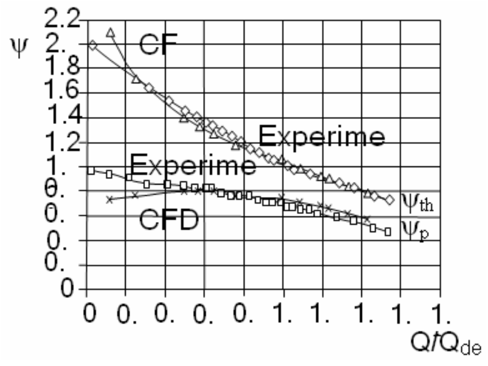


Fig. 13. Comparison between results obtained from experiment and CFD [11].

The theoretical head coefficient obtained can be compared with that obtained from Eq. (5).

In the present study, the experimental work was not carried on. But, results from a previous study reported in the literature [11] show good agreement between the theoretical head coefficient and the static pressure rise coefficient. However, due to recirculation, agreement becomes worst at very low ($Q/Q_{design}$). An example of the comparison obtained from [11] is shown in Fig. 13.

## 8. Conclusion

In the impeller analysis with CFD software, it was found that the suitable mesh number was more than 50,000 nodes. The turbulence model and turbulence intensity yielded similar results at the same condition. The prediction of impeller performance indicated that the loss coefficient was minimum and the hydraulic efficiency was maximum at a volumetric flow rate $Q/Q_{design} = 0.7$. The total head rise values gained from the analysis were acceptably non-significantly different from the head at the design point. The surface roughness value was found to have a high effect on loss. That is, at higher surface roughness, the value of the loss coefficient was also found to increase. The loss coefficient of the impeller is 0.015 when $0.6 < Q/Q_{design} < 1.2$. Maximum hydraulic efficiency of impeller is 0.98 at $Q/Q_{design} = 0.7$.

## Acknowledgments

The present study was supported financially by the Thailand Research Fund (TRF). Their guidance and assistance are gratefully acknowledged. The authors would like to express their appreciation to Professor J. F. Guelich, of the Laboratory for Hydraulic Machines, Ecole Polytechnique Federale de Lausanne, Switzerland, for his valuable comments and suggestions.

## Nomenclature

B : Width at the exit of the impeller (mm.)
$C_{m2}$ : Meridian component of absolute velocity at exit (m/s)
$C_{U1}$ : Circumferential component of absolute velocity at inlet (m/s)
$C_{U2}$ : Circumferential component of absolute velocity at exit (m/s)
FEA : Finite element analysis
g : Gravitational acceleration (m/s$^2$)
H : Design head of the impeller (m)

$H_p$ : Measured static pressure head (m)
$H_{th}$ : Theoretical head (m)
$H_{tot}$ : Total head of pump (m)
k : Turbulence kinetic energy
l : Circumference of the impeller exit on rotational polar coordinate for each blade impeller (mm.)
$N_s$ : Specific speed (1/min)
P : Pressure (N/m$^2$)
$P_{er}$ : Power losses by component of axial thrust balance device (kW)
$P_m$ : Mechanical power losses (kW)
$P_{RR}$ : Disk friction power (kW)
$P_{s3}$ : Power losses dissipated in inter-stage seal (kW)
$P_w$ : Water horse power (kW)
$P_{1static}$ : Static pressure at the impeller inlet (N/m$^2$)
$P_{2static}$ : Static pressure at the impeller exit (N/m$^2$)
$P_{1total}$ : Total pressure at the impeller inlet (N/m$^2$)
$P_{2total}$ : Total pressure at the impeller exit (N/m$^2$)
Q : Any volumetric flow rate (m$^3$/s)
$Q_{design}$ : Volumetric flow rate at the design point (m$^3$/s)
$Q_E$ : Leakage flow through axial thrust balance device (m$^3$/s)
$Q_h$ : Leakage flow through auxiliaries (m$^3$/s)
$Q_{sp}$ : Leakage flow through seal at impeller inlet (m$^3$/s)
RNG : Renormalization group
r : Radius from the reference point (m)
U : Circumferential velocity (m/s)
$U_2$ : Impeller tip speed (m/s)
$\vec{V}$ : Velocity vector (m/s)
y : Any distance along the circumference of the exit measured on rotational polar coordinate (mm.)
z : Any distance along the width at the exit of impeller measured from Hub to Shroud (mm.)
$Z_{La}$ : Hydraulic losses of the impeller
$\eta$ : Efficiency of pump
$\eta_h$ : Hydraulic efficiency of the impeller
$\mu$ : Absolute viscosity (kg/m-s)
$\rho$ : Density of medium (kg/m$^3$)
$\Omega$ : Angular velocity (rad/s)
$\varepsilon$ : Turbulence eddy dissipation
$\omega$ : Turbulent frequency
$\psi$ : Head coefficient
$\psi_p$ : Static pressure rise coefficient of the impeller
$\psi_{LA}$ : Total head rise coefficient of the impeller
$\psi_{th}$ : Theoretical head coefficient
$\zeta_{LA}$ : Impeller loss coefficient
$\vec{\nabla}$ : Operator $\equiv i\frac{\partial}{\partial x} + j\frac{\partial}{\partial y} + k\frac{\partial}{\partial z}$

## References


[1] P. Cooper and E. Graf, Computational fluid dynamical analysis of complex internal flows in centrifugal pump, *Proceedings of the 11th International Pump Users Symposium*, Houston, USA, (1994), 83-93.

[2] FC. Visser, Some user experience demonstrating the use of CFD for cavitation analysis and head prediction of centrifugal pump, *Proceedings of the ASME Fluids Engineering Division Summer Meeting (FEDSM'01)*, New Orleans, La, USA, May-June (2001), paper FEDSM2001-18087.

[3] E. Blanco-Marigorta, J. Fernandez-Francos, J. L. Parrondo-Gayo and C. Santolaria-Marros, Numerical simulation of centrifugal pumps, *Proceedings of the ASME Fluids Engineering Division Summer Meeting (FEDSM'00)*, Boston, Mass, USA, June (2000), paper FEDSM00- 11162.

[4] J. Gonzalez, J. Fernandez-Francos, E. Blanco and C. Santolaria-Marros, Numerical simulation of the dynamic effects due to impeller-volute interaction in a centrifugal pump,*Transactions of the ASME, Journal of Fluids Engineering*, 124 (2002) 348-355.

[5] J. L. Parrondo-Gayo, J. Gonzalez-Perez and J. Fernandez-Francos, The effect of the operating point on the pressure fluctuations at the blade passage frequency in the volute of a centrifugal pump, *Transactions of the ASME, Journal of Fluids Engineering*, 124 (2002) 784-794.

[6] F. Gu, A. Engeda, M. Cave and J. L. Di Liberti, A numerical investigation on the volute/diffuser interaction due to the axial distortion at the impeller exit, *Transactions of the ASME, Journal of Fluids Engineering*, 123 (2001) 475-483.

[7] F. Muggli, P. Holbein and P. Dupont, CFD calculation of a mixed flow pump characteristic from shutoff to maximum flow, *Proceedings of the ASME Fluids Engineering Division Summer Meeting (FEDSM'01)*, New Orleans, La, USA, May-June (2001), paper FEDSM2001-18072.

[8] C. Cravero and M. Marini, Modeling of incompressible three-dimensional flow in rotating turbomachinery passages, *Proceedings of the ASME Fluids Engineering Division Summer Meeting (FEDSM'02)*, Montreal, Quebec, Canada, July (2002), paper FEDSM2002-31177.

[9] J. F. Guelich, J. N. Favre and K. Denus, An assessment of pump impeller performance predictions by 3D-Navier Stokes calculations, P*roceedings of the*

*ASME Fluids Engineering Division Summer Meeting (FEDSM'97)*, Vancouver, Canada, June 1997, paper FEDSM1997-3341.

[10] M. Asueje, F. Bakir, S. Kouidri, F. Kenyery and R. Rey, Numerical Modelisation of the Flow in Centrifugal Pump: *Volute Influence in Velocity and Pressure Fields, International Journal of Rotating Machinery*, 3 (2005) 244-255.

[11] J. F. Guelich, *Kreiselpumpen*, Springer, Berlin, 2004 (in German).

**Somchai Wongwises** is currently a Professor of Mechanical Engineering at King Mongkut's University of Technology Thonburi, Bangmod, Thailand. He received his Doktor Ingenieur (Dr.Ing.) in Mechanical Engineering from the University of Hannover, Germany, in 1994. His research interests include two-phase flow, heat transfer enhancement, and thermal system design. Professor Wongwises is the head of the Fluid Mechanics, Thermal Engineering and Two-Phase Flow Research Laboratory (FUTURE).

**Suthep Kaewnai** obtained a B. S. degree in Mechanical Engineering, 1980 from the King Monkut's University of Technology Thonburi and M. S. degree in Mechanical Engineering, 1983 from Chulalongkorn University. He is currently an assistant professor at King  Mongkut's University of Technology Thonburi. Suthep's research interests are in the area of pumps and small hydroturbine.

**Manuspong Chamaoot** received a B. S. degree ,1972 and M.S. degree in Mechanical Engineering, 1979 from the King Monkut's University of Technology Thonburi. He is currently an assistant professor at King Monkut's University of Technology Thonburi. His research interests are in the field of mechanical vibration for rotating equipment and computational fluid dynamics.